International Journal of Antimicrobial Agents 53 (2019) 795–804

Contents lists available at ScienceDirect

International Journal of Antimicrobial Agents

journal homepage: www.elsevier.com/locate/ijantimicag

Comprehensive proteomic and metabolomic profiling of *mcr-1*-mediated colistin resistance in *Escherichia coli*

Hui Li[a,b,1], Yingyu Wang[a,1], Qingshi Meng[c,1], Yang Wang[d], Guoliang Xia[e], Xi Xia[a,*], Jianzhong Shen[a,**]

[a] Beijing Advanced Innovation Center for Food Nutrition and Human Health, College of Veterinary Medicine, China Agricultural University, Beijing, China
[b] Beijing Key Laboratory of Diagnostic and Traceability Technologies for Food Poisoning, Beijing Center for Disease Prevention and Control, Beijing, China
[c] State Key Laboratory of Animal Nutrition, Institute of Animal Science, Chinese Academy of Agricultural Sciences, Beijing, China
[d] Beijing Key Laboratory of Detection Technology for Animal-Derived Food Safety, China Agricultural University, Beijing, China
[e] State Key Laboratory of Agrobiotechnology, College of Biological Science, China Agricultural University, Beijing, China

ARTICLE INFO

Article history:
Received 22 October 2018
Accepted 16 February 2019

Editor: Jean-Marc Rolain

Keywords:
mcr-1
Colistin
Proteomic
Metabolomic
Antimicrobial resistance

ABSTRACT

Spread of the *mcr-1* gene in human and veterinary medicine has jeopardised the use of polymyxins, last-resort antibiotics against life-threatening multidrug-resistant Gram-negative bacteria. As a lipid-modifying gene, whether *mcr-1* causes proteomic and metabolomic changes in bacteria and affects the corresponding metabolic pathway is largely unknown. In this study, label-free quantitative proteomics and untargeted metabolomics were used to profile comprehensive proteome and metabolome characteristics of *mcr-1*-mediated colistin-resistant and -susceptible *Escherichia coli* in order to gain further insight into the colistin resistance mechanism. Large sets of differentially expressed proteins (DEPs) and metabolites were identified that contributed to *mcr-1*-mediated antimicrobial resistance, predominantly in different growth conditions with and without colistin. *mcr-1* caused downregulated expression of most proteins in order to adapt to drug pressure. Pathway analysis showed that metabolic processes were significantly affected, mainly related to glycerophospholipid metabolism, thiamine metabolism and lipopolysaccharide (LPS) biosynthesis. The substrate phosphoethanolamine (PEA) for *mcr-1* to mediate colistin resistance was accumulated in colistin-resistant *E. coli*. Notably, *mcr-1* not only caused PEA modification of the bacterial cell membrane lipid A but also affected the biosynthesis and transport of lipoprotein in colistin resistance by disturbing the expression of efflux pump proteins involved in the cationic antimicrobial peptide (CAMP) resistance pathway. Overall, disturbed glycerophospholipid metabolism and LPS biosynthesis as well as accumulation of the substrate PEA was closely related with *mcr-1*-mediated colistin resistance. These findings could provide further valuable information to inhibit colistin resistance by blocking this metabolic process.

1. Introduction

Resistance to polymyxins has emerged worldwide, threatening the efficacy of the last-resort antimicrobials used for the treatment of multidrug-resistant Enterobacteriaceae infections in humans [1,2]. In parallel, heavy use of colistin in veterinary medicine is currently being re-evaluated owing to increased reports of colistin-resistant bacteria, and colistin was banned as a feed additive in China in 2016 [3]. Colistin resistance can be mediated by phosphoethanolamine (PEA) or 4-amino-arabinose modification of lipid A that abolishes the initial electrostatic interaction with polymyxins [4,5]. Colistin resistance appeared in multidrug-resistant bacteria owing to with chromosomal mutations in lipid A biosynthesis and regulatory genes and, more recently, in isolates with the mobile colistin resistance determinants *mcr-1 to -8* [6–13]. *mcr-1* is a recently reported plasmid-mediated colistin resistance gene but it actually existed years previously [14]. The *mcr-1* gene encodes a member of the family of PEA transferases that decorate the lipid A headgroups of lipopolysaccharide (LPS) with PEA [6,15]. The rate of *mcr-1*-mediated resistance increased rapidly and the gene may be acquired by humans from the food chain, constituting a serious threat to public health [14,16,17].

Since *mcr-1* was first reported, many studies clearly clarified the current situation of its transmission and provided epidemic evidence in food, livestock and humans [17–19]. How to

* Corresponding author. Tel.: +86 10 6273 2803; fax: +86 10 6273 1032.
** Co-corresponding author.
E-mail addresses: xxia@cau.edu.cn (X. Xia), sjz@cau.edu.cn (J. Shen).
[1] These three authors contributed equally to this work.

https://doi.org/10.1016/j.ijantimicag.2019.02.014
0924-8579/

effectively avoid the public-health hazard caused by *mcr-1* has become an important challenge. In an effort to address these matters and to increase the metabolic coverage of available methodologies, system-level approaches have been applied in unknown functional discovery. Proteomics and metabolomics, as new 'omic' techniques, can study the entire protein expression and dynamic changes of metabolites in specific tissues or cells on a system level, and elucidate the developmental process of specific biological processes and regulatory mechanisms [20,21]. In addition, use of proteomics techniques to study bacterial resistance mechanisms makes it possible to find potential large-scale targets for antimicrobials [22,23]. Fernández-Reyes et al. studied the resistance cost of colistin-resistant *Acinetobacter baumannii* and found that outer membrane proteins, chaperones, protein biosynthesis factors and metabolic enzymes were downregulated in colistin-resistant strains from a proteomic perspective [24]. It is noteworthy that the fatty acyl side chain with the C_{12}–C_{14} carbon chain of the lipid A group, which is essential for the maintenance of bacterial LPS function, is involved in the bacterial fatty acid type II synthesis pathway, suggesting that it is essential in order to decipher the mechanism of *mcr-1*-mediated resistance from a metabolic perspective. However, as a lipid-modifying gene, comprehensive proteomic and metabolomic profiling of *mcr-1*-mediated colistin resistance in bacteria is still unknown.

In this study, the comprehensive proteome and metabolome changes in *mcr-1*-mediated colistin-resistant and -susceptible *Escherichia coli* strains were investigated using label-free quantitative proteomics and untargeted metabolomics. Differentially expressed proteins (DEPs) and metabolites were successfully selected to decipher in-depth the colistin resistance mechanisms mediated by *mcr-1*. This study could provide insight into the molecular mechanisms and potential disturbed metabolic pathways of *mcr-1*-mediated bacterial resistance.

2. Materials and methods

2.1. Strains, plasmid construction and antimicrobial susceptibility testing

The *mcr-1* gene with its own promoter (156 bp) and downstream sequence (111 bp) was amplified by PCR from plasmid pHNSHP45 [6] using Q5 High-Fidelity DNA Polymerase (New England Biolabs, Ipswich, MA) and was cloned into plasmid pUC19 using *Eco*RI and *Xba*I sites. The constructed plasmid pUC19-*mcr-1* was then transformed into DH5α competent *E. coli* cells. Transformants were selected by the inclusion of ampicillin (100 μg/mL) on Luria broth (LB) agar plates. Cloning results were confirmed by PCR sequencing. Successfully constructed *E. coli* DH5α(pUC19-*mcr-1*) carrying a 1893-bp fragment was used as the engineering strain. The blank plasmid pUC19 was chemically transformed into *E. coli* DH5α and was considered as the control strain [*E. coli* DH5α(pUC19)]. Antimicrobial susceptibility testing was performed on the abovementioned constructed *mcr-1*-expressing strains and control strains against polymyxin B and colistin according to Clinical and Laboratory Standards Institute (CLSI) guidelines [25]. Minimum inhibitory concentrations (MICs) of *E. coli* DH5α(pUC19-*mcr-1*) for colistin and polymyxin B were 4 μg/mL, representing an eight-fold increase compared with the control strain.

2.2. Protein lysis and digestion

Colistin-resistant *E. coli* DH5α(pUC19-*mcr-1*) was grown in LB supplemented with colistin and polymyxin B under three different drug culture conditions (0, 0.5 and 1 μg/mL), respectively. The control strain was cultured overnight in blank LB at 37°C until exponential growth phase. Three biological replicates were performed for each culture condition. Cells were centrifugated at 10 000 × *g* at 4°C for 30 min and were washed twice with 10 mL of ice-cold phosphate-buffered saline (PBS). The cells were then re-suspended in 1 mL of lysis buffer [8 M urea, 50 mM Tris–HCl (pH 7.4), 0.5% sodium dodecyl sulfate (SDS), 1 mM phenylmethanesulfonyl fluoride (PMSF), 20 μL protease inhibitor cocktail]. Cells were lysed by indirect sonication (35% energy, 4 min) in a Sonics VCX105 (Sonics & Materials, Inc., Newtown, CT) and were centrifuged at 20 000 × *g* at 4°C for 30 min. A small aliquot of the supernatant was taken to determine the protein concentration using a Pierce BCA Protein Assay Kit (Thermo Fisher Scientific, Rockford, IL). A total of 100 μg of protein was taken and was added to 0.1 M triethylammonium bicarbonate (TEAB) to a final volume of 100 μL. The protein was reduced with a final concentration of 50 mM dithiothreitol buffer at 37°C for 1 h and was alkylated with iodoacetamide (100 mM final concentration) in the dark for 30 min. Five volumes of cold acetone (–20°C) were added for protein precipitation and the solution was incubated overnight at –20°C. Following centrifugation at 20 000 × *g* for 20 min, the precipitate was left at room temperature for 2–3 min until acetone volatilisation. Then, 100 μL of 0.1 M TEAB was added to dissolve the protein. Trypsin (2 μg) in 0.1 M TEAB was added to digest the protein and was incubated at 37°C for 16 h. Following digestion, the sample was evacuated in a SpeedVac® rotary evaporator (Thermo Fisher Scientific, Japan). The solution was reconstituted with 100 μL of water/acetonitrile (98/2 v/v, containing 0.1% formic acid) and was drained again until almost no white salt was visible in the microcentrifuge tube. Peptides were dissolved in 100 μL of water/acetonitrile (98/2 v/v, containing 0.1% formic acid) and were centrifuged at 20 000 × *g* for 15 min. The supernatant was collected and was injected onto a nano liquid chromatography–tandem mass spectrometry (NanoLC-MS) analysis system.

2.3. Label-free quantitative proteome analysis

Label-free quantitative proteome analysis was performed using an Eksigent NanoLC®-2D coupled with a TripleTOF® 6600 mass spectrometer (Sciex Inc., Framingham, MA). Peptides were first loaded on a trap column ChromXP C_{18}-CL resin (200 μm × 0.5 mm, 3 μm, 120 Å) and were then separated on a cHiPLC column ChromXP C_{18}-CL resin (75 μm × 15 cm, 3 μm, 120 Å). The flow rate was 300 nL/min over a 95-min multisegment gradient on mobile phase A (water:dimethyl sulfoxide:acetonitrile 96:2:2 v/v/v, containing 0.1% formic acid) and mobile phase B (acetonitrile:dimethyl sulfoxide:water 96:2:2 v/v/v, containing 0.1% formic acid). The gradient elutions were optimised as follows: 0–50 min, 5% to 20% B; 50–70 min, 20% to 32% B; 70–75 min, 32% to 80% B; 75–80 min, 80% B; and 80–95 min, 80% to 5% B.

For data-dependent acquisition, a TOF-MS scan over a mass range *m/z* 350–1500 Da with 250 ms accumulation time, followed by *m/z* 100–1800 Da for MS/MS scans in high sensitivity mode with 80 ms accumulation time of up to TOF 40 ion candidates per cycle was performed. For data-independent acquisition, a set of 25 overlapping transmission windows, each 25 Da wide, was constructed and covered the precursor mass range of *m/z* 400–1000 Da. The SWATH product ion scans were acquired in the range of *m/z* 100–1800 Da. The SWATH-MS1 survey scan was acquired with an accumulation time of 50 ms and was followed by 40 ms accumulation time high sensitivity product ion scans.

Data analysis was performed using Skyline [26]. ProteinPilot v.5.0 software was utilised to carry out spectral counting for label-free quantification. DEPs were filtered by the following cut-off: false discovery rate, <1%; peptide confidence threshold, >99%; fold change, ≥2.0; and *P*-value, <0.01.

2.4. Reverse transcription quantitative PCR (RT-qPCR)

A total of 14 DEPs (*tolA, yqaB, nadC, ybiG, htp, glpQ, osmY, waaJ, yaaF, eutE, ydcH, yjiY, gutD* and *yccX*) were verified by RT-qPCR using iQ™ SYBR® Green SuperMix (QIAGEN) and were analysed using a 7500 Real-Time PCR system (Applied Biosystems, Thermo Fisher Scientific, Inc.). The primer sequences are given in Supplementary Table S1. Relative expression of these selected genes was normalised to expression of the 16S rRNA gene. Amplification efficiency and relative transcript abundance were analysed using the $2^{-\Delta\Delta CT}$ method and *t*-test.

2.5. LC/MS metabolomic analysis

Colistin-susceptible *E. coli* DH5α(pUC19) was cultured overnight in blank LB at 37°C, and colistin-resistant *E. coli* DH5α(pUC19-*mcr-1*) was grown in LB medium under three different culture concentrations of colistin (0, 0.5 and 1 μg/mL; CST0, CST0.5 and CST1, respectively). Bacterial turbidity was adjusted to an optical density at 600 nm (OD_{600}) of 0.8 using blank sterile LB. Then, 10 mL aliquots were directly transferred to 50 mL tubes and were pelleted by fast centrifugation (5 min at 10 000 × *g*, 0°C). The supernatant was discarded and the pellets were flash frozen in liquid nitrogen to quench cell metabolism. Subsequently, the cell pellet was extracted with 1.5 mL of methanol at −20°C and was vortexed for 1 min. The freeze–thawing operation in liquid nitrogen was repeated three times to lyse the cells. Samples were centrifuged at 12 000 × *g* for 15 min at −10°C (Beckman Coulter Inc., USA) and the cellular metabolites were re-extracted again using the above procedure. Cellular extracts were combined and dried under vacuum using a SpeedVac® V100 (Thermo Fisher Scientific, Inc.). The extracted metabolites were re-suspended in 500 μL of acetronile:water (50:50 v/v, containing 0.1% formic acid). A quality control (QC) sample was prepared by mixing aliquots from all supernatant samples (50 μL from each sample). Mixed standard solution (sulfadiazine, difloxacin, monensin, tylosin and thiamphenicol) at final concentrations of 200 ng/mL was spiked into the extracts for QC purposes of compound mass.

Cellular metabolites were analysed using a Waters ACQUITY ultra-high performance liquid chromatography (UPLC) system coupled with a hybrid TOF-MS SYNAPT HDMS (Waters, Manchester, UK). The weakly polar metabolites were separated by BEH Shield RP C_{18} column (50 × 2.1 mm, 1.7 μm) with mobile phase A (0.1% formic acid in water) and mobile phase B (0.1% formic acid in acetonitrile) at a flow rate of 0.3 mL/min at 35°C. The optimised gradient elution procedure was as follows: 0–1 min, 2% to 5% B; 1–8 min, 5% to 90% B; 8–10 min, 90% to 100% B; 10–12 min, 100% to 2% B. The strongly polar metabolites were analysed by BEH HILIC column (50 × 2.1 mm, 1.7 μm) and were eluted using mobile phase A (acetonitrile:water 95:5 v/v, containing 0.05 mM ammonium acetate) and mobile phase B (acetonitrile:water 50:50 v/v, containing 0.05 mM ammonium acetate) at a flow rate of 0.3 mL/min at 35°C. The gradient elution conditions were optimised as follows: 0–1 min, 1% B; 1–2 min, 1% to 10% B; 2–4 min, 10% B; 4–5 min, 10% to 30% B; 5–7 min, 30% B; 7–8.5 min, 30% to 50% B; 8.5–10 min, 50% to 100% B; 10–12 min, 100% to 1% B. QTOF/MS spectrum was operated in ESI^+ and ESI^- modes, respectively. The mass range was set at *m/z* 50–1200 Da in the full-scan mode. The optimised ESI parameters were as follows: capillary voltage, 3.0 kV; cone voltage, 35 V; source temperature, 100°C; desolvation temperature, 450°C; and desolvation gas flow, 600 L/h. For accurate mass measurement, leucine enkephalin was used as the lock spray standard ($[M+H]^+$ =556.2771; $[M-H]^-$ =554.2615) at a concentration of 100 ng/mL with a flow rate of 50 μL/min.

The data sets were processed using Progenesis QI v.2.3 software (Nonlinear Dynamics Ltd., Newcastle, UK). Multivariate analysis, including principal component analysis (PCA) and partial least squares discriminant analysis, was constructed to determine the distributions and to find the metabolic differences between the control and resistant strains. The filtered data ($P < 0.05$ and fold change ≥2) were processed for further analysis and display. The assigned modified metabolite ions were identified by database searches in the ECMDB (http://www.ecmdb.ca), ChemSpider (http://www.chemspider.com/), HMDB (http://www.hmdb.ca/) and METLIN (https://metlin.scripps.edu/) databases. The mass tolerance for the database search was set at 10 ppm.

2.6. Data analysis

The metabolic pathways of DEPs and differential metabolites were analysed using KEGG software (http://www.genome.jp/kegg/) to investigate the disturbed metabolic pathways and to facilitate biological interpretation. The DEPs, metabolites and corresponding pathways were imported into Cytoscape software v.3.4.0 for visualisation of the network models. A heat map was constructed with R software v.3.4.4 to show the key information related to comprehensive changes induced by the *mcr-1* gene in colistin resistance.

3. Results

3.1. Comprehensive proteome changes under different drug culture conditions

To define proteome changes accompanying *mcr-1*-mediated colistin resistance, protein levels of colistin-resistant and -susceptible *E. coli* strains in different culture conditions were compared using label-free quantitative proteomics. A total of 2784 proteins were identified, representing ca. 64.3% coverage of the predicted *E. coli* proteome. The protein distribution detected in the colistin-resistant *E. coli* DH5α(pUC19-*mcr-1*) proteome using SWATH-MS is shown in Fig. 1A. A total of 57 proteins (26 upregulated and 31 downregulated) were differentially expressed when no drug was added in the medium (CST/PMB0 in Fig. 1B; Supplementary Table S2). When *E. coli* DH5α(pUC19-*mcr-1*) was grown under different selection pressure of colistin and polymyxin B (0.5 μg/mL and 1 μg/mL), the number of DEPs was increased and most of the proteins were downregulated (CST0.5/1 and PMB0.5/1 in Fig. 1B; Supplementary Tables S3–S6). Resistant *E. coli* DH5α carrying *mcr-1* against colistin and polymyxin B showed similar changes. A Venn diagram of DEPs in *E. coli* DH5α(pUC19-*mcr-1*) showed that up to 16 DEPs including membrane proteins (OmpX, RbsB, OmpT and YtfJ), metabolic enzymes (Maa, IscU, YbiV, TreF, ThiG, AzoR, MsrC and GcvH), DNA repair helicase (DinG) and uncharacterised proteins (YdcH, YdeI and YbgS) appeared simultaneously in the CST (CST0.5 and CST1) and PMB (PMB0.5 and PMB1) groups (Fig. 1C). GO analysis of DEPs whose abundance increased in different culture conditions found significant enrichment of categories consistent with the key biological events related to antimicrobial resistance. Observed categories such as metabolic processes, biosynthesis of secondary metabolites and biosynthesis of amino acids are shown in Fig. 1D. The variation trend of DEPs under the selection pressure of colistin and polymyxin B was then compared. Under the condition of colistin, among all 57 DEPs, 26 proteins showed consistent changes, of which 11 were downregulated and 15 were upregulated. Under the condition of polymyxin B, a total of 22 proteins among 57 DEPs showed consistent changes, of which 10 were downregulated and 12 were upregulated. It was interesting to note that although most proteins were downregulated in the presence of polymyxins, proteins that were initially differently expressed in *E. coli* carrying the *mcr-1* gene and were also differently expressed in the presence of antibiotics were mostly upregulated. Among

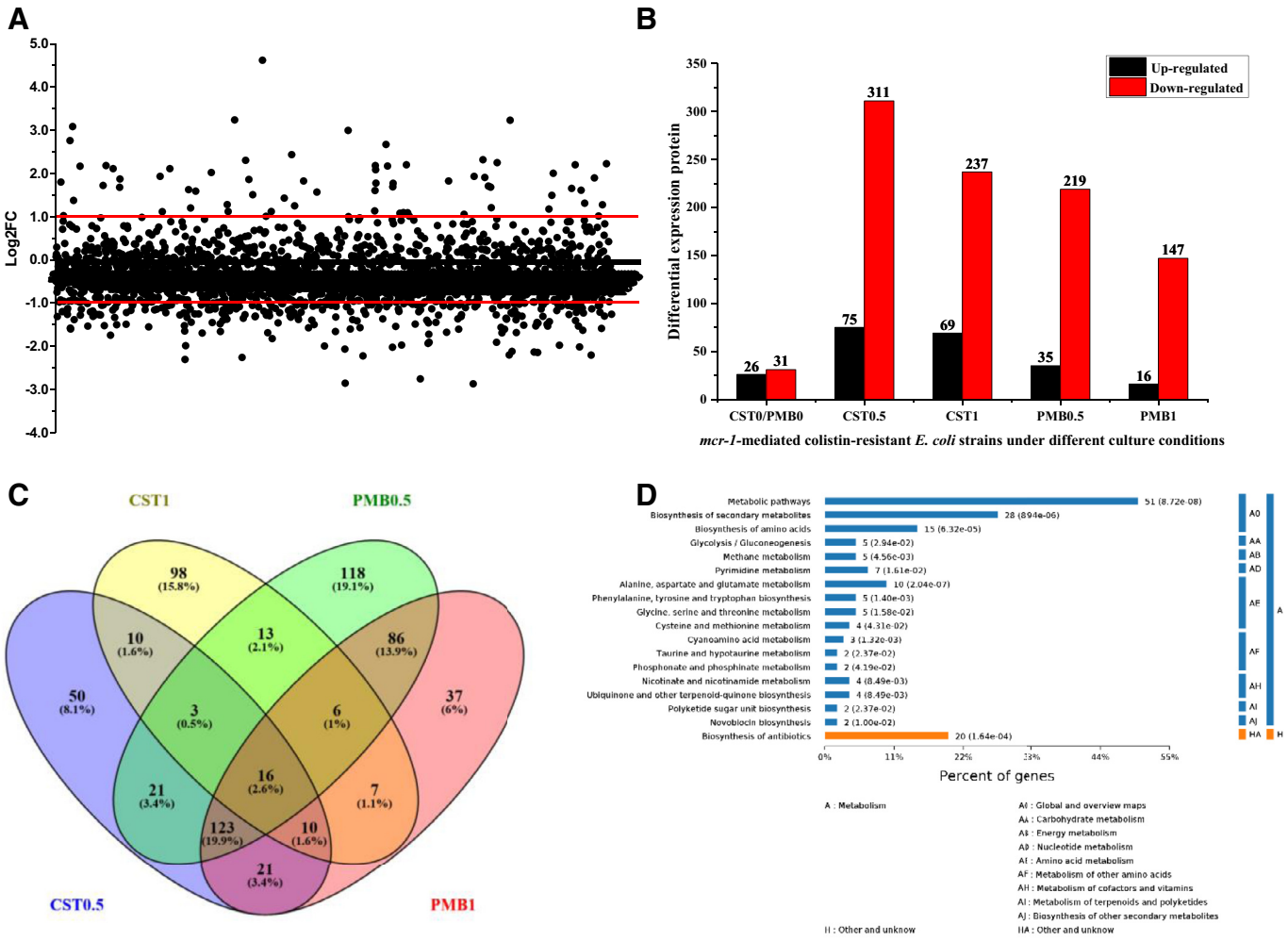

Fig. 1. Comprehensive proteome profiles induced by the *mcr-1* gene using label-free quantitative proteomics. (A) Protein distribution detected in colistin-resistant *Escherichia coli* DH5α(pUC19-*mcr-1*) proteome using SWATH-MS. (B) Bar diagram reflecting the number of upregulated and downregulated proteins in *E. coli* DH5α(pUC19-*mcr-1*) under different selection pressures of colistin and polymyxin B: CST0/PMB0, no-drug group; CST0.5 and CST1, colistin 0.5 μg/mL and 1 μg/mL; and PMB0.5 and PMB1, polymyxin B 0.5 μg/mL and 1 μg/mL. (C) Venn diagram of differentially expressed proteins (DEPs) in *E. coli* DH5α(pUC19-*mcr-1*) under different selection pressure of colistin and polymyxin B. (D) Metabolic pathways enriched with DEPs identified in colistin-resistant *E. coli* DH5α(pUC19-*mcr-1*) without the addition of drug.

all of the proteins with the same changes, 14 proteins simultaneously appeared in three different drug culture conditions including PMB0/CST0, CST0.5 and PMB0.5, of which 5 proteins (TolA, YqaB, NadC, YbiG and Htp) were downregulated and 9 proteins (GlpQ, OsmY, WaaJ, YaaF, EutE, YdcH, YjiY, GutD and YccX) were upregulated.

Gene expression of these 14 consistent DEPs was then investigated using RT-qPCR (Fig. 2). Gene expression of *htp, nadC, tolA, ybiG* and *yqaB* was downregulated and was consistent with the proteomic analysis. However, expression of these genes was upregulated in the presence of colistin and polymyxin B 1 μg/mL. Compared with the gene expression of *tolA* in colistin-susceptible *E. coli* DH5α(pUC19), its expression decreased by 0.08-, 0.20- and 0.19-fold, respectively, in colistin-resistant *E. coli* DH5α(pUC19-*mcr-1*) cultured in colistin (CST0, CST0.5 and CST1). Furthermore, the relative expression of *yjiY, eutE, glpQ, gutD, osmY, waaJ, yaaF, yccX* and *ydcH* was significantly upregulated in *E. coli* DH5α(pUC19-*mcr-1*) compared with their expression in the control strain *E. coli* DH5α(pUC19) not carrying the *mcr-1* gene. Noteworthy, *ydcH, osmY* and *tolA* had the most significant changes ($P < 0.01$) in gene expression, demonstrating that these three proteins might play an important role in *mcr-1*-mediated drug resistance.

3.2. Functional analysis of proteins altered during antibiotic pressure

Pathway analysis of DEPs found that lysine biosynthesis, pyruvate metabolism and peptidoglycan biosynthesis were altered in colistin-resistant *E. coli* DH5α(pUC19-*mcr-1*) when no drug was added in the medium. Further analysis demonstrated that the number of proteins involved in LPS biosynthesis was increased (up to 5-fold) when 0.5 μg/mL colistin was added. However, the amount of protein involved in the synthesis of LPS was decreased as the drug concentration continued to increase to 1 μg/mL. Similar changes could also be confirmed in the cationic antimicrobial peptide (CAMP) resistance, peptidoglycan biosynthesis and glycerophospholipid metabolic pathways. Similarly, changes in thiamine metabolism, phenylalanine, tyrosine and tryptophan biosynthesis as well as pyruvate metabolic processes were also largely affected (Fig. 3). It was noteworthy that expression of GlpQ, EutB, PgpC, PlsB, Cdh, UgpQ, Aas, EutC and GlpC involved in glycerophospholipid metabolism were upregulated in colistin-resistant *E. coli* DH5α(pUC19-*mcr-1*) under the selection pressure of colistin.

Under different concentrations of polymyxin B selection pressure, DEPs showed the same trend in expression and the proteins involved in metabolic processes varied greatly. These metabolic processes mainly referred to glycerophospholipid metabolism,

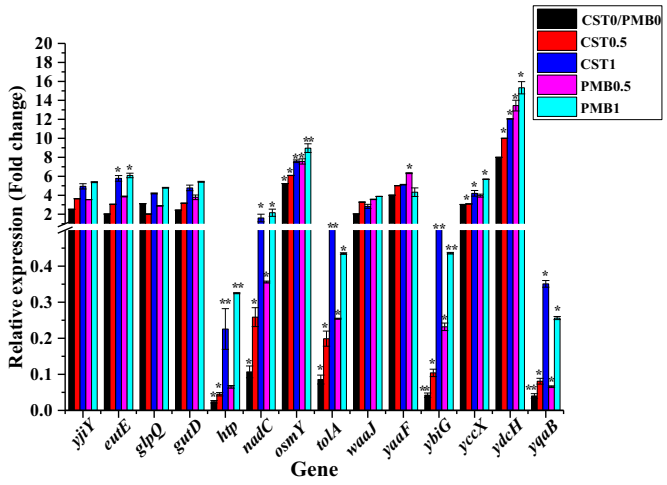

Fig. 2. Transcript levels of 14 proteins appeared simultaneously under different selection pressures of colistin and polymyxin. 16S rRNA was used as an internal control. All samples were prepared in three biological replicates. Error bars represented the standard error of the mean. Data are normalised to the susceptible strain *E. coli* DH5α(pUC19). * $P < 0.05$ and ** $P < 0.01$ compared with the susceptible strain. CST0/PMB0, no-drug group; CST0.5 and CST1, colistin 0.5 μg/mL and 1 μg/mL; and PMB0.5 and PMB1, polymyxin B 0.5 μg/mL and 1 μg/mL.

thiamine metabolism, LPS biosynthesis and CAMP resistance (Fig. 3). However, there was no change in the relevant proteins involved in CAMP resistance following the addition of polymyxin B to the culture medium, unlike colistin. In addition, the number of DEPs affecting the function of ribosomal proteins was increased with increasing drug concentration, indicating that the protein synthesis process has been affected. Bacteria were required to enhance protein synthesis in order to adapt to drug selection pressure. In terms of energy metabolism, part of the proteins involved in the tricarboxylic acid cycle (TCA) cycle and pentose phosphate pathway were upregulated, indicating an increase in energy metabolism to accommodate drug stress (Fig. 3).

3.3. Untargeted metabolomic analysis

Untargeted metabolomic profiling of colistin-resistant *E. coli* DH5α(pUC19-*mcr-1*) and colistin-susceptible *E. coli* DH5α(pUC19) strains under different culture conditions was studied to determine their metabolic characteristics. First, PCA was used to investigate the metabolomic profile of the two strains cultured in different concentrations of colistin. PCA analysis separated on a BEH RP C_{18} chromatographic column in ESI^+ and ESI^- mode are shown in Fig. 4A and Fig. 4C, respectively. The intracellular metabolites between the two strains cultured in different drug concentrations differed. Clustering analysis of any pair of comparisons in their respective space was obvious. Orthogonal projection to latent structures discriminant analysis was then applied to identify the main difference variables. S-plots of the metabolites separated on BEH RP C_{18} column in ESI^+ and ESI^- mode are shown in Fig. 4B and Fig. 4D, respectively. A total of 67 differential metabolites were simultaneously found in different drug culture conditions, of which 49 metabolites were selected in ESI^+ mode and 18 metabolites were found in ESI^- mode (Table 1). Among all of the identified metabolites separated on C_{18} column, 11 features (10 upregulated and 1 downregulated) were found in ESI^+ mode and 13 features (10 upregulated and 3 downregulated) were selected in ESI^- mode, respectively. The metabolites were then analysed separated on an HILIC column. A total of 38 compounds (18 upregulated and 20 downregulated) were identified in ESI^+ mode and 5 features (4 upregulated and 1 downregulated) were selected in ESI^- mode, respectively (Table 1). For QC purposes, several reference standards were added to verify the reliability of the metabolomic analysis. The average error of calculated mass was below 10 ppm, the retention time was nearly identical, and the relative standard deviation (RSD) of the peak area in three batches (different extracts) was 3.52–6.24% (Supplementary Table S7).

3.4. Enrichment and metabolic pathway analysis

A heatmap representation of all identified intracellular differential metabolites from the colistin culture group (CST0,

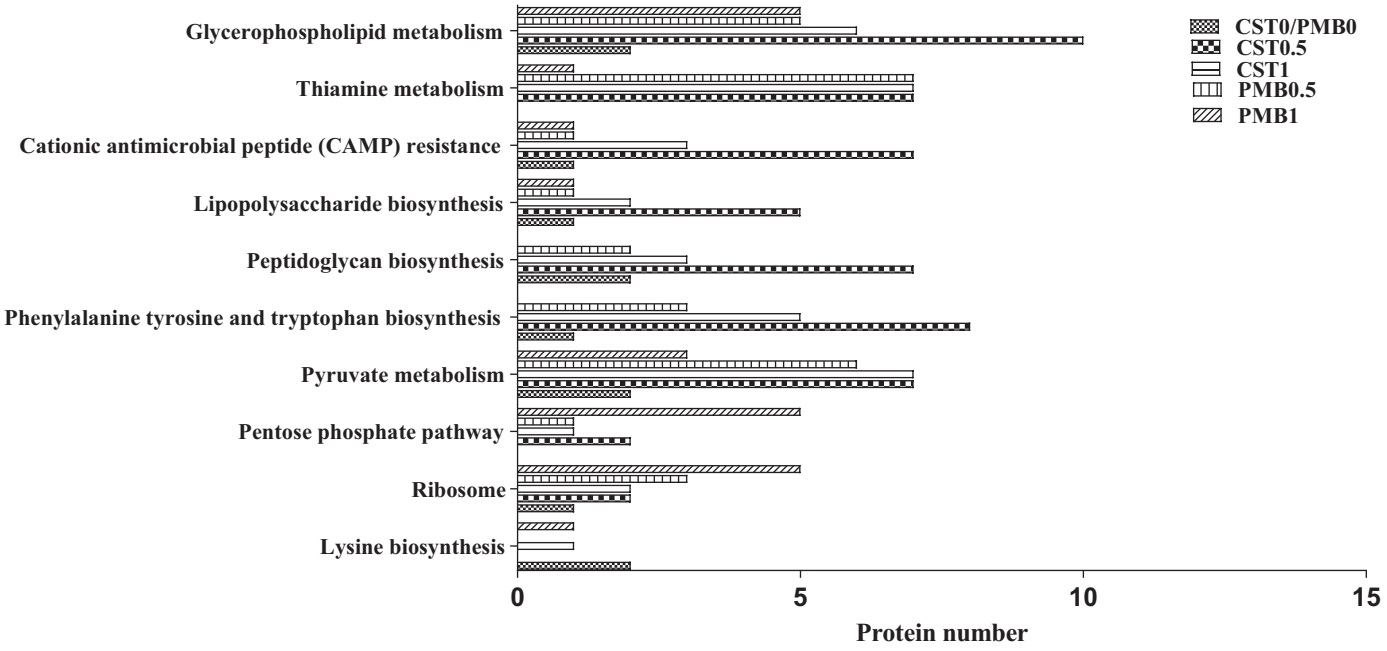

Fig. 3. KEGG pathway analysis of differentially expressed proteins (DEPs) in *Escherichia coli* DH5α(pUC19-*mcr-1*) under different selection pressures of colistin and polymyxin B. Each column represents the protein number involved in the related metabolic pathway. CST0/PMB0, no-drug group; CST0.5 and CST1, colistin 0.5 μg/mL and 1 μg/mL; and PMB0.5 and PMB1, polymyxin B 0.5 μg/mL and 1 μg/mL.

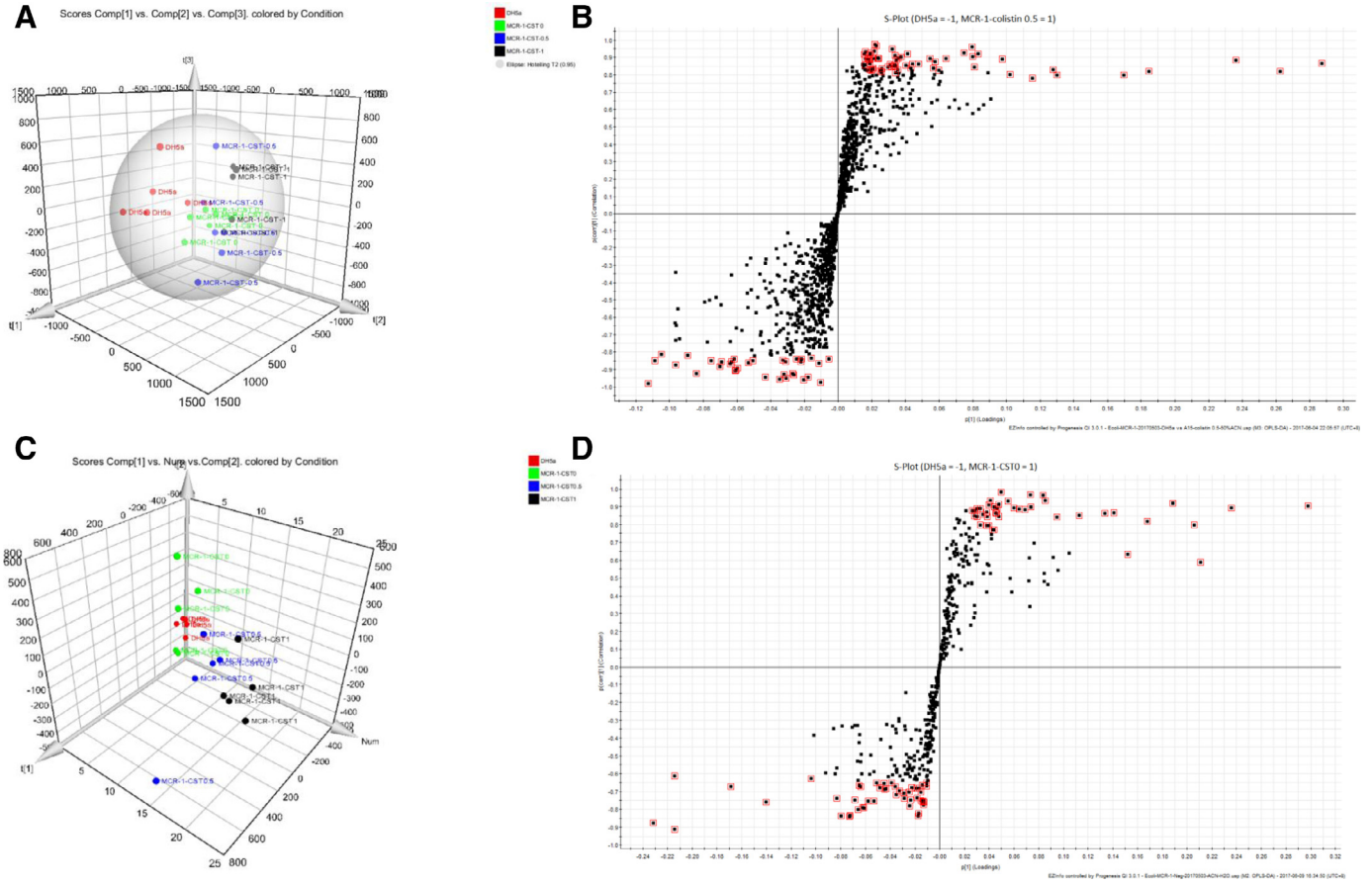

Fig. 4. Metabolic characteristic of the cellular metabolites of colistin-susceptible and -resistant *Escherichia coli* strains under different concentrations of colistin separated on a BEH C_{18} column. (A,C) Principal component analysis of microbial extracts from resistant and susceptible strains in ESI^+ mode (A) and ESI^- mode (C). (B,D) Representative S-plot of resistant strains versus susceptible strains in ESI^+ mode (B) and ESI^- mode (D).

CST0.5 and CST1) is shown in Fig. 5A. Metabolite set enrichment analysis showed that pantothenate and CoA biosynthesis, glycerolipid metabolism and phosphatidylethanolamine biosynthesis contributed to *mcr-1*-mediated bacterial metabolism (Fig. 5B). Metabolic pathway analysis was then performed and it was found that polyketide sugar unit biosynthesis, glycerophospholipid metabolism and lysine biosynthesis were significantly enriched for all of the identified differential metabolites (Fig. 5C). Interestingly, protein–metabolite interaction analysis of the disturbed glycerophospholipid metabolism in *mcr-1*-mediated colistin resistance by the integration of proteomics and metabolomics found that a high number of differential metabolites including PE(14:1(9Z)/16:1(9Z)), GPEtn(18:1(9Z)/0:0), LysoPE(0:0/15:0), GPEtn(18:1(9Z)/0:0), PE(16:1(9Z)/18:1(11Z)), PE(18:1(11Z)/17:0), PE(22:4(7Z,10Z,13Z,16Z)/P-18:0), PGP(16:1(9Z)/12:0), sn-glycerol-1-phosphate, 1-acyl-sn-glycero-3-phosphoglycerol (N-C14:1) and 1-acyl-sn-glycero-3-phosphoglycerol (N-C16:1) involved in glycerophospholipid metabolism were upregulated in *E. coli* DH5α(pUC19-*mcr-1*) compared with *E. coli* DH5α(pUC19) (Fig. 5D).

4. Discussion

As known, the colistin resistance mechanism of *mcr-1* is that the inner membrane protein MCR-1 chemically modifies the lipid A of bacterial LPS with PEA [27–29]. As a lipid-modifying gene, whether *mcr-1* causes comprehensive proteomic and metabolomic changes in bacteria and affects the corresponding metabolic pathway is largely unknown. This study is the first to investigate the comprehensive proteomic and metabolomic profiles of *mcr-1*-mediated colistin-resistant and -susceptible *E. coli* strains under different selection pressures of colistin and polymyxin B.

It is well established that polymyxins exert their antimicrobial activity mainly through disruption of the bacterial outer membrane [30,31]. In the current study, a label-free quantitative proteomics approach was used to elucidate the protein profiles of colistin-resistant *E. coli* DH5α carrying *mcr-1* and it was found that colistin and polymyxin B caused *mcr-1*-mediated resistant bacteria to exhibit different proteome profiles (Fig. 1D). This suggested that colistin-resistant bacteria might alter their metabolism to adapt to antibiotic resistance. Proteomic characteristics showed that *mcr-1* caused disturbed metabolic regulation such as glycerophospholipid metabolism, thiamine metabolism, LPS biosynthesis and CAMP resistance (Fig. 3), and the protein profile of *E. coli* carrying *mcr-1* to colistin showed the most significant changes, which is consistent with the report of Hua et al. [32]. Integrative proteomic and metabolomic analysis demonstrated that GlpQ and EutE involved in glycerophospholipid metabolism were significantly upregulated in colistin-resistant *E. coli* DH5α(pUC19-*mcr-1*) under the condition of blank LB broth. However, the number of DEPs (GlpQ, EutB, PgpC, PlsB, Cdh, UgpQ, Aas, EutC and GlpC) involved in glycerophospholipid metabolism increased when the resistant *E. coli* DH5α(pUC19-*mcr-1*) was cultured in different drug conditions. In addition, metabolite expression analysis found that the metabolites involved in glycerophospholipid metabolism were upregulated due to the insertion of *mcr-1*. Remarkably, the substrate PEA (KEGG ID: C00350) for *mcr-1* to mediate colistin resistance was investigated as a differential metabolite and its expression under different colistin selection pressure (CST0, CST0.5 and CST1) was upregulated in

Table 1
Putative differential metabolites identified in colistin-resistant *Escherichia coli* DH5α(pUC19-*mcr-1*) under three different drug culture conditions

Mode	RT (min)	Mass	Compound ID	Description	Adducts	Formula	ANOVA (*P*-value)	Fold change		
								CST0	CST0.5	CST1
C_{18} (ESI^+)	Upregulated									
	8.47	485.2964	HMDB0093047	DG(12:0/14:0/0:0)	M+H	$C_{29}H_{56}O_5$	0.009185	3.29	2.97	4.07
	8.47	133.0988	C00077	Ornithine	M+H-2H_2O	$C_5H_{12}N_2O_2$	0.012675	2.55	2.36	3.68
	10.90	660.4632	C00350	PE(14:1(9Z)/16:1(9Z))	M+H	$C_{35}H_{66}NO_8P$	0.004749	2.84	3.52	3.59
	7.58	353.3034	C00681	1-Dodecanoyl-sn-glycerol 3-phosphate	M+H	$C_{15}H_{29}O_7P$	0.000477	2.18	2.04	2.88
	7.14	339.2882	HMDB0032112	1,2,4-Nonadecanetriol	M+Na	$C_{19}H_{40}O_3$	6.70E-07	4.72	5.17	4.36
	7.14	480.3109[a]	C00416	GPEtn(18:1(9Z)/0:0)	M+H	$C_{23}H_{46}NO_7P$	7.85E-06	3.63	4.79	4.04
	6.44	452.2795[a]	HMDB0035366	Cytochalasin Opho	M+H	$C_{28}H_{37}NO_4$	1.86E-05	2.87	4.38	3.44
	6.44	311.2572	HMDB0031060	(R)-2-Hydroxysterculic acid	M+H	$C_{19}H_{34}O_3$	1.84E-05	2.70	3.79	3.13
	6.58	434.2660	HMDB0033870	Butanamide	M+H	$C_{23}H_{35}N_3O_5$	0.000115	2.29	3.65	2.68
	14.03	424.3612		NI			0.00079	2.21	2.97	3.56
	Downregulated									
	6.75	223.0621	CSID58167740	3-Nitro-N'-[(E)-2H-pyrrol-2-ylidene methyl]benzohydrazide	M+H-2H_2O	$C_{12}H_{10}N_4O_3$	5.32E-07	-3.01	-3.14	-4.03
C_{18} (ESI^-)	Upregulated									
	1.09	565.0495	C00029	UDP-glucose	M-H	$C_{15}H_{24}N_2O_{17}P_2$	6.86E-06	3.40	5.10	4.64
	1.09	606.0750	C00203	Uridine diphosphate-N-acetylgalactosamine	M-H	$C_{17}H_{27}N_3O_{17}P_2$	0.000277	2.99	3.84	3.60
	1.60	545.0585	C11907	4,6-Dideoxy-4-oxo-dTDP-D-glucose	M-H	$C_{16}H_{24}N_2O_{15}P_2$	0.000133	4.13	4.33	5.46
	1.60	563.0693	C00842	dTDP-D-glucose	M-H	$C_{16}H_{26}N_2O_{16}P_2$	3.76E-05	3.38	4.59	3.81
	1.66	547.0739	C03319	Deoxythymidine diphosphate-l-rhamnose	M-H	$C_{16}H_{26}N_2O_{15}P_2$	1.92E-07	2.01	2.52	2.06
	2.22	686.1423	C00882	Dephospho-CoA	M-H	$C_{21}H_{35}N_7O_{13}P_2S$	5.25E-05	3.94	3.04	2.35
	4.89	438.2624	HMDB0011472	LysoPE(0:0/15:0)	M-H	$C_{20}H_{42}NO_7P$	0.021843	2.08	2.82	2.58
	5.24	478.2961[a]	C00416	GPEtn(18:1(9Z)/0:0)	M-H	$C_{23}H_{46}NO_7P$	4.24E-06	2.47	4.18	3.40
	4.78	450.2659[a]	HMDB0035366	Cytochalasin Opho	M-H	$C_{28}H_{37}NO_4$	3.85E-05	2.19	3.83	2.93
	1.93	602.1158		NI			0.000166	19.96	20.24	17.21
	Downregulated									
	1.71	524.6228		NI			1.57E-05	-3.21	-3.60	-4.33
	3.82	145.9300	C00047	L-Lysine	M-H	$C_6H_{14}N_2O_2$	7.71E-08	-3.80	-4.19	-5.89
	1.71	525.1245	C05817	(1R,6R)-6-Hydroxy-2-succinylcyclohexa-2,4-diene-1-carboxylate	2M+FA-H	$C_{11}H_{12}O_6$	0.000155	-3.26	-3.56	-4.33
HILIC (ESI^+)	Upregulated									
	5.37	140.0560	C03283	(2S)-2,4-Diaminobutanoate	M+H	$C_4H_9N_2O_2$	7.62E-09	8.13	10.87	10.81
	6.73	162.0977	C00956	Aminoadipic acid	M+H	$C_6H_{11}NO_4$	2.41E-10	4.49	4.40	5.04
	6.16	163.9947	CSID7822055	2-{[(2R)-2-Hydroxypropyl]sulfanyl} ethanesulfonate	M+H-2H_2O	$C_5H_{11}O_4S_2$	0.003684	8.42	20.16	15.60
	1.86	244.0810	HMDB0060478	Gamma-glutamyl-beta-cyanoalanine	M+H	$C_9H_{13}N_3O_5$	1.40E-07	2.64	2.42	2.75
	5.37	257.1383	HMDB0031772	1-Methoxy-1-(2,4,5-trimethoxyphenyl)-2-propanol	M+H	$C_{13}H_{20}O_5$	2.32E-05	16.59	16.35	16.36
	4.00	311.2477	CSID22146489	2-{4-[4-(Cyclopentyloxy)benzyl]-1-isopropyl-2-piperazinyl}ethanol	M+H-2H_2O	$C_{21}H_{34}N_2O_2$	0.000324	2.30	3.53	2.33
	3.90	339.2795	C04677	5′-P-Ribosyl-5-amino-4-imidazole carboxamide	M+H	$C_9H_{15}N_4O_8P$	2.81E-05	3.03	6.23	4.48
	3.17	353.2589	CSID392311	(1S)-4-{[Ammonio(imino)methyl] amino}-1-carboxy-1-butanaminium	2M+H	$C_6H_{16}N_4O_2$	6.18E-06	3.66	3.95	3.89
	3.17	381.2918	C00416	1-Tetradecanoyl-sn-glycerol 3-phosphate	M+H	$C_{17}H_{33}O_7P$	0.000541	20.09	19.96	19.20
	5.55	474.9170		NI			0.000152	23.23	24.29	24.57
	3.15	509.4552	C12298	3,7-Dimethyl-6-octen-1-yl hexanoate	2M+H	$C_{16}H_{30}O_2$	0.019951	3.90	5.00	6.41
	1.41	547.4762	C11907	4,6-Dideoxy-4-oxo-dTDP-D-glucose	M+H	$C_{16}H_{24}N_2O_{15}P_2$	0.006269	2.34	6.26	35.13
	3.07	561.4923	C07040	Hydrabamine	M+H-2H_2O	$C_{42}H_{64}N_2$	0.01040	2.18	2.45	2.51
	3.04	575.5169	C03541	Tetrahydrofolyl-[Glu]	M+H	$C_{24}H_{30}N_8O_9$	6.29E-06	3.57	3.66	3.36
	3.04	716.5437	C00350	PE(16:1(9Z)/18:1(11Z))	M+H	$C_{39}H_{74}NO_8P$	2.27E-05	3.48	3.38	3.36
	3.16	732.5395	C00350	PE(18:1(11Z)/17:0)	M+H	$C_{40}H_{78}NO_8P$	0.001257	7.41	7.30	7.02
	3.02	744.5699	C00350	PE(22:4(7Z,10Z,13Z,16Z)/P-18:0)	M+H-2H_2O	$C_{45}H_{82}NO_7P$	0.000392	3.03	3.05	2.48
	6.37	745.3891	CSID30792055	PGP(16:1(9Z)/12:0)	M+H	$C_{34}H_{66}O_{13}P_2$	0.002629	39.49	3.90	15.72

(*continued on next page*)

Table 1 (*continued*)

Mode	RT (min)	Mass	Compound ID	Description	Adducts	Formula	ANOVA (*P*-value)	Fold change		
								CST0	CST0.5	CST1
	Downregulated									
	5.62	90.9634	C00209	Oxalic acid	M+H	$C_2H_2O_4$	8.43E-06	-2.57	-2.75	-2.84
	5.62	104.9790	C06001	3-Hydroxyisobutyric acid	M+H	$C_4H_8O_3$	2.09E-05	-2.58	-2.82	-2.24
	5.51	134.0050	HMDB0000191	L-Aspartic acid	M+H	$C_4H_7NO_4$	0.000107	-3.52	-4.09	-4.09
	5.60	158.9505	C00337	4,5-Dihydroorotic acid	M+H	$C_5H_6N_2O_4$	1.56E-05	-2.54	-2.79	-2.77
	5.62	172.9665	C03892	Sn-Glycerol-1-phosphate	M+H	$C_3H_9O_6P$	1.42E-05	-2.8	-2.82	-2.36
	5.62	176.0524	CSID3400747	N-Cyclopropyl-4-methylbenzenesulfonamide	M+H-2H_2O	$C_{10}H_{13}NO_2S$	0.000414	-3.41	-4.10	-4.16
	5.63	186.9822	C00597	3-Phosphoglycerate	M+H	$C_3H_7O_7P$	8.98E-05	-2.68	-2.61	-2.53
	5.62	226.9393	C00251	Chorismate	M+H-2H_2O	$C_{10}H_{10}O_6$	8.11E-06	-2.42	-2.64	-2.73
	5.62	240.9558	C00491	L-Cystine	M+H	$C_6H_{12}N_2O_4S_2$	1.21E-05	-2.58	-2.32	-2.54
	5.65	254.9715	HMDB0003229	9-hexadecenoic acid	M+H	$C_{16}H_{30}O_2$	2.55E-05	-2.59	-2.71	-2.37
	5.69	268.9873	C11544	2(alpha-D-mannosyl)-D-glycerate	M+H-2H_2O	$C_9H_{16}O_9$	5.77E-05	-3.03	-3.02	-3.07
	5.65	308.9442	–	alpha-D-Ribose 1-methylphosphonate 5-phosphate	M+H	$C_6H_{14}O_{10}P_2$	3.79E-06	-3.77	-3.44	-3.72
	5.59	362.9183	–	Octadecanoyl-phosphate (n-C18:0)	M+H-2H_2O	$C_{18}H_{35}O_5P$	0.00309	-2.01	-2.29	-2.38
	5.62	376.9344	HMDB0000095	Cytidine monophosphate	M+H	$C_{11}H_{15}Cl_2O_2PS_3$	8.04E-05	-3.00	-2.26	-2.47
	5.69	418.9828	C04823	(*S*)-2-[5-amino-1-(5-phospho-D-ribosyl)imidazole-4-carboxamido]succinate	M+H	$C_{13}H_{19}N_4O_{12}P$	0.000404	-3.55	-2.91	-2.90
	5.59	430.9082		NI			1.80E-05	-2.69	-2.32	-2.45
	5.60	444.9250	C00700	Xanthosine diphosphate	M+H	$C_{10}H_{14}N_4O_{12}P_2$	0.000117	-4.25	-2.32	-3.23
	5.62	458.9416	C00692	UDP-N-Acetylmuramoyl-L-alanyl-D-glutamate	M+H	$C_{22}H_{32}Cl_2N_2O_4$	2.39E-05	-2.87	-2.36	-2.55
	5.65	472.9580	C00081	Inosine triphosphate	M+H-2H_2O	$C_{10}H_{15}N_4O_{14}P_3$	5.21E-05	-3.05	-2.38	-2.68
	5.68	526.9322	C00842	dTDP-D-Glucose	M+H-2H_2O	$C_{16}H_{24}N_2O_{16}P_2$	0.000182	-41.53	-10.8	-18.58
HILIC (ESI^-)	Upregulated									
	4.71	282.2693	HMDB0000827	octadecanoic acid	M-H	$C_{18}H_{35}O_2$	6.29E-05	2.40	2.69	2.43
	3.92	322.2150	CSID34448528	(3R,5R)-7-[(1S,2S,4aR,6R,8aS)-2,6-Dimethyl-1,2,4a,5,6,7,8,8a-octahydro-1-naphthalenyl]-3,5-dihydroxyheptanoate	M-H	$C_{19}H_{31}O_4$	4.61E-05	2.65	3.91	3.98
	4.85	451.8983	C18126	1-Acyl-sn-glycero-3-phosphoglycerol (N-C14:1)	M-H	$C_{20}H_{38}O_9P$	0.024623	3.75	4.94	5.68
	4.71	480.0320	C18126	1-Acyl-sn-glycero-3-phosphoglycerol (N-C16:1)	M-H	$C_{22}H_{42}O_9P$	0.00022	6.36	7.96	2.35
	Down-regulated									
	1.50	635.7543	HMDB0007160	DG(18:0/19:1(9Z)/0:0)	M-H	$C_{40}H_{76}O_5$	4.46E-06	-2.65	-6.18	-5.14

CST0/PMB0, no-drug group; CST0.5 and CST1, colistin 0.5 μg/mL and 1 μg/mL; and PMB0.5 and PMB1, polymyxin B 0.5 μg/mL and 1 μg/mL; NA, not identified.
[a] Differential metabolites identified both in ESI^+ and ESI^- mode separated on BEH C_{18} column.

resistant *E. coli* DH5α(pUC19-*mcr-1*). It was predicted that accumulation of PEA occurred in *mcr-1*-mediated colistin resistance in *E. coli*. Glycerophospholipids are important membrane lipids in bacteria and play a vital role in cellular functions, including the regulation of transport processes, protein function and signal transduction [33]. In addition, glycerophospholipids are essential components of lipoproteins and influence their function and metabolism [34]. These results demonstrated that *mcr-1* caused a disturbed glycerophospholipid metabolism pathway to adapt to colistin selection pressure in *E. coli*.

In addition to the effect on membrane lipids, *mcr-1* caused metabolic perturbation of LPS biosynthesis in colistin-resistant strains. LPS is a key component of the outer membrane, a permeability barrier in Gram-negative bacteria, in which it plays an important role in its integrity [35,36]. When *E. coli* strains carrying *mcr-1* were cultured under the selection pressure of colistin and polymyxin B, the expression of seven members (LpxC, KdsA, KdtA, RfaI, RfaJ, lpp and LptB) of the LPS transport protein family that together transport LPS from the inner membrane to the outer leaflet of the outer membrane were decreased in *mcr-1*-mediated colistin-resistant *E. coli*. So we predicted that *mcr-1* might influence the biosynthesis and transport of lipoprotein in colistin resistance.

Furthermore, colistin and polymyxin B also brought changes in the relevant efflux proteins. Efflux pumps could form multicomponent 'pumps' that span both the inner and outer membranes in Gram-negative bacteria and confer resistance to a broad range of antibiotics [37,38]. Expression of efflux pump components is jointly controlled by several positive global regulators, which respectively decrease and enhance the transcription of specific genes, such as *acrAB–tolC* [39]. Insertion of *mcr-1* in *E. coli* not only caused PEA modification of bacterial cell membrane lipid A, but also affected the efflux of polymyxins by disturbing the expression of efflux pump proteins involved in the CAMP resistance pathway. Baron and Rolain found that the efflux pump inhibitor carbonyl cyanide *m*-chlorophenyl hydrazone (CCCP) could restore colistin susceptibility in *mcr-1* plasmid-mediated colistin-resistant strains [40], supporting our finding that efflux pumps might play a role in colistin resistance in Mcr-1-producing *E. coli*.

In addition, the number of DEPs affecting ribosomal function was increased in *E. coli* DH5α(pUC19-*mcr-1*) with increasing polymyxin B concentration, indicating that the protein synthesis process has been disturbed. The bacteria could enhance protein synthesis in order to adapt to drug selection pressure. In terms of energy metabolism, part of the proteins involved in the TCA

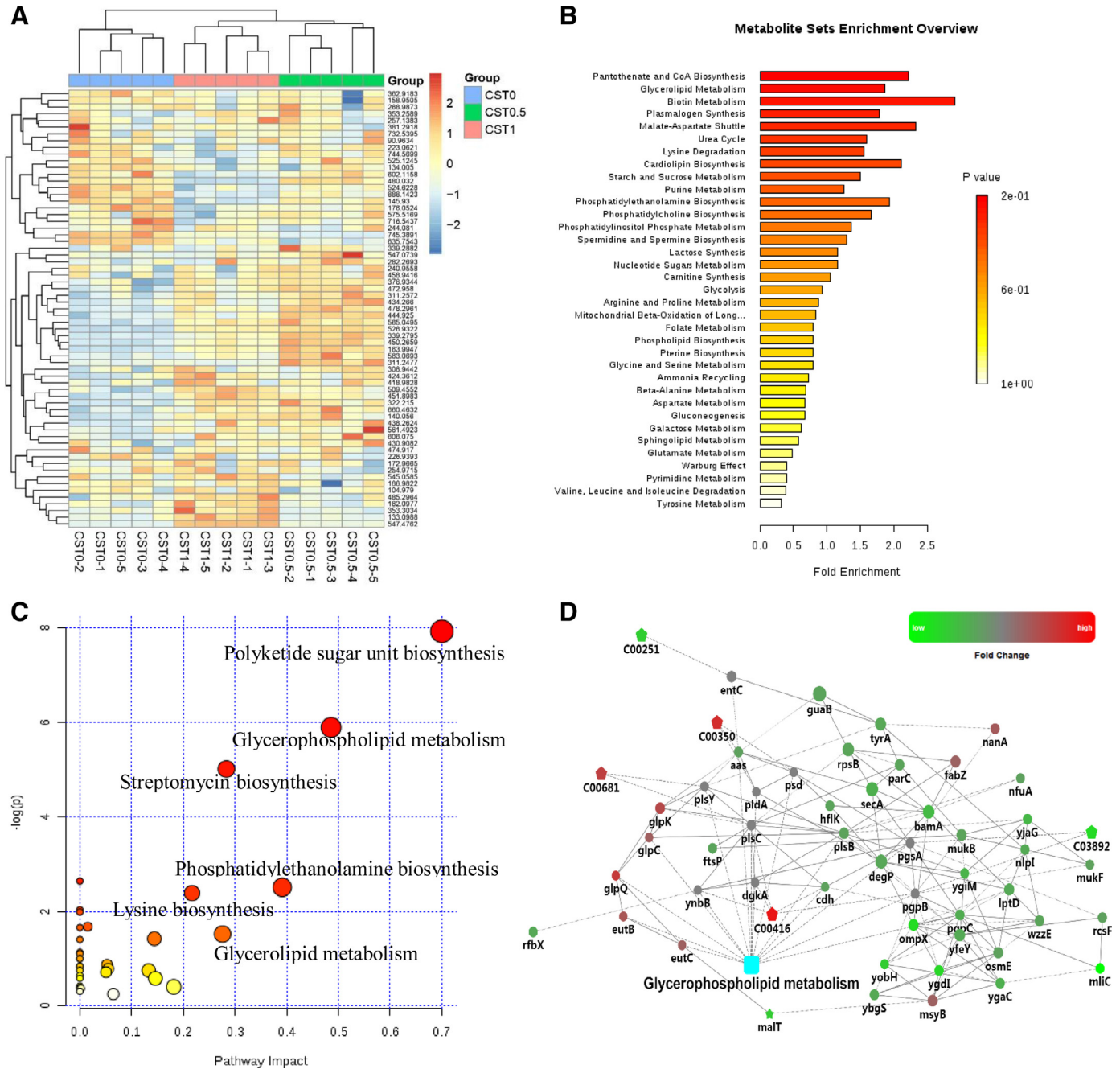

Fig. 5. Enrichment and metabolic pathway analysis of *mcr-1*-mediated colistin resistance using untargeted metabolomics. (A) Heat map representation of intracellular metabolic profiles from *Escherichia coli* DH5α(pUC19-*mcr-1*) under different concentrations of colistin culture conditions (CST0, CST0.5 and CST1). Each column represents one biological replicate, and each row represents one targeted metabolite detected in this study. (B) Metabolite set enrichment analysis showed that pantothenate and CoA biosynthesis, glycerophospholipid metabolism, glycerolipid metabolism and phosphatidylethanolamine biosynthesis contributed to *mcr-1*-mediated bacterial disturbed metabolism. (C) Visualisation of disturbed metabolic pathways in *mcr-1*-mediated colistin-resistant strains. (D) Protein–metabolite interaction analysis of the disturbed glycerophospholipid metabolism in *mcr-1*-mediated colistin resistance by the integration of proteomics and metabolomics. CST0/PMB0, no-drug group; CST0.5 and CST1, colistin 0.5 μg/mL and 1 μg/mL; and PMB0.5 and PMB1, polymyxin B 0.5 μg/mL and 1 μg/mL. Rectangular nodes represent KEGG pathway; round nodes indicate protein; pentagons represent metabolites. Red, upregulated; green, downregulated.

cycle and pentose phosphate pathway were upregulated, indicating an increase in energy metabolism to accommodate drug stress. Increased metabolic activity and energy production are required for pathogens to resist high antibiotic stress [41]. The metabolic changes may be a consequence of the biological cost of antibiotic resistance. Lysine biosynthesis is critical for protein biosynthesis and a component of the peptidoglycan layer of bacterial cell walls [42]. Metabolomic analysis found that expression of lysine and L-2-aminoadipate was downregulated in colistin-resistant *E. coli* DH5α(pUC19-*mcr-1*) compared with the susceptible strain.

In conclusion, the current data highlight the comprehensive proteome and metabolome profiling of *mcr-1*-mediated colistin resistance in *E. coli*. Different proteome characteristics were exhibited under different selection pressure of colistin and polymyxin B. The substrate PEA for *mcr-1* to mediate colistin resistance was accumulated in colistin-resistant *E. coli*. Notably, *mcr-1* not only caused PEA modification of bacterial cell membrane lipid A but also affected the efflux of colistin by disturbing the expression of efflux pump proteins involved in the CAMP resistance pathway. Furthermore, the disturbed glycerophospholipid metabolism was closely

related with *mcr-1*-mediated colistin resistance and this finding could further provide valuable information to inhibit colistin resistance by blocking this metabolic process.

Funding

This work was supported by the National Natural Science Foundation of China [grant no. 31602107] and the Capital Health Research and Development of Special Funding [grant no. 2018-4-3017].

Competing interests

None declared.

Ethical approval

Not required.

Supplementary materials

Supplementary material associated with this article can be found, in the online version, at doi:10.1016/j.ijantimicag.2019.02.014.

References

[1] Li J, Nation RL, Turnidge JD, Milne RW, Coulthard K, Rayner CR, et al. Colistin: the re-emerging antibiotic for multidrug-resistant Gram-negative bacterial infections. Lancet Infect Dis 2006;6:589–601.
[2] Bialvaei AZ, Samadi Kafil H. Colistin, mechanisms and prevalence of resistance. Curr Med Res Opin 2015;31:707–21.
[3] Walsh TR, Wu Y. China bans colistin as a feed additive for animals. Lancet Infect Dis 2016;16:1102–3.
[4] Poirel L, Jayol A, Nordmann P. Polymyxins: antibacterial activity, susceptibility testing, and resistance mechanisms encoded by plasmids or chromosomes. Clin Microbiol Rev 2017;30:557–96.
[5] Anandan A, Evans GL, Condic-Jurkic K, O'Mara ML, John CM, Phillips NJ, et al. Structure of a lipid A phosphoethanolamine transferase suggests how conformational changes govern substrate binding. Proc Natl Acad Sci U S A 2017;114:2218–23.
[6] Liu Y-Y, Wang Y, Walsh TR, Yi L-X, Zhang R, Spencer J, et al. Emergence of plasmid-mediated colistin resistance mechanism MCR-1 in animals and human beings in China: a microbiological and molecular biological study. Lancet Infect Dis 2016;16:161–8.
[7] Xavier BB, Lammens C, Ruhal R, Kumar-Singh S, Butaye P, Goossens H, et al. Identification of a novel plasmid-mediated colistin-resistance gene, *mcr-2*, in *Escherichia coli*, Belgium, June 2016. Euro Surveill 2016;21. doi:10.2807/1560-7917.ES.2016.21.27.30280.
[8] Yin W, Li H, Shen Y, Liu Z, Wang S, Shen Z, et al. Novel plasmid-mediated colistin resistance gene *mcr-3* in *Escherichia coli*. mBio 2017;8 e00543-17.
[9] Borowiak M, Fischer J, Hammerl JA, Hendriksen RS, Szabo I, Malorny B. Identification of a novel transposon-associated phosphoethanolamine transferase gene, *mcr-5*, conferring colistin resistance in D-tartrate fermenting *Salmonella enterica* subsp. *enterica* serovar Paratyphi B. J Antimicrob Chemother 2017;72:3317–24.
[10] Carattoli A, Villa L, Feudi C, Curcio L, Orsini S, Luppi A, et al. Novel plasmid–mediated colistin resistance *mcr-4* gene in *Salmonella* and *Escherichia coli*, Italy 2013, Spain and Belgium, 2015 to 2016. Euro Surveill 2017;22 pii:30589.
[11] AbuOun M, Stubberfield EJ, Duggett NA, Kirchner M, Dormer L, Nunez-Garcia J, et al. *mcr-1* and *mcr-2* variant genes identified in *Moraxella* species isolated from pigs in Great Britain from 2014 to 2015. J Antimicrob Chemother 2017;72:2745–9.
[12] Yang YQ, Li YX, Lei CW, Zhang AY, Wang HN. Novel plasmid-mediated colistin resistance gene *mcr-7.1* in *Klebsiella pneumoniae*. J Antimicrob Chemother 2018;73:1791–5.
[13] Wang X, Wang Y, Zhou Y, Li J, Yin W, Wang S, et al. Emergence of a novel mobile colistin resistance gene, *mcr-8*, in NDM-producing *Klebsiella pneumoniae*. Emerg Microbes Infect 2018;7:122.
[14] Shen Z, Wang Y, Shen Y, Shen J, Wu C. Early emergence of *mcr-1* in *Escherichia coli* from food-producing animals. Lancet Infect Dis 2016;16:293.
[15] Hinchliffe P, Yang QE, Portal E, Young T, Li H, Tooke CL, et al. Insights into the mechanistic basis of plasmid-mediated colistin resistance from crystal structures of the catalytic domain of MCR-1. Sci Rep 2017;7:39392–401.
[16] Wang Y, Zhang R, Li J, Wu Z, Yin W, Schwarz S, et al. Comprehensive resistome analysis reveals the prevalence of NDM and MCR-1 in Chinese poultry production. Nat Microbiol 2017;2:16260.
[17] Shen Y, Zhou H, Xu J, Wang Y, Zhang Q, Walsh TR, et al. Anthropogenic and environmental factors associated with high incidence of *mcr-1* carriage in humans across China. Nat Microbiol 2018;3:1054–62.
[18] Feng Y. Transferability of MCR-1/2 polymyxin resistance: complex dissemination and genetic mechanism. ACS Infect Dis 2018;4:291–300.
[19] Caniaux I, van Belkum A, Zambardi G, Poirel L, Gros MF. MCR: modern colistin resistance. Eur J Clin Microbiol Infect Dis 2017;36:415–20.
[20] Pérez-Llarena FJ, Bou G. Proteomics as a tool for studying bacterial virulence and antimicrobial resistance. Front Microbiol 2016;7:410.
[21] Jozefczuk S, Klie S, Catchpole G, Szymanski J, Cuadros-Inostroza A, Steinhauser D, et al. Metabolomic and transcriptomic stress response of *Escherichia coli*. Mol Syst Biol 2010;6:364.
[22] Lima TB, Pinto MF, Ribeiro SM, de Lima LA, Viana JC, Gomes Junior N, et al. Bacterial resistance mechanism: what proteomics can elucidate. FASEB J 2013;27:1291–303.
[23] Vranakis I, Goniotakis I, Psaroulaki A, Sandalakis V, Tselentis Y, Gevaert K, et al. Proteome studies of bacterial antibiotic resistance mechanisms. J Proteomics 2014;97:88–99.
[24] Fernández-Reyes M, Rodríguez-Falcón M, Chiva C, Pachón J, Andreu D, Rivas L. The cost of resistance to colistin in *Acinetobacter baumannii*: a proteomic perspective. Proteomics 2009;9:1632–45.
[25] Clinical and Laboratory Standards Institute. Performance standards for antimicrobial disk and dilution susceptibility tests for bacteria isolated from animals. 3rd ed. Wayne, PA: CLSI; 2015. Documents M31-A3 and VET01S.
[26] MacLean B, Tomazela DM, Shulman N, Chambers M, Finney GL, Frewen B, et al. Skyline: an open source document editor for creating and analyzing targeted proteomics experiments. Bioinformatics 2010;26:966–8.
[27] Sun J, Zhang H, Liu YH, Feng Y. Towards understanding MCR-like colistin resistance. Trends Microbiol 2018;26:794–808.
[28] Stojanoski V, Sankaran B, Prasad BV, Poirel L, Nordmann P, Palzkill T. Structure of the catalytic domain of the colistin resistance enzyme MCR-1. BMC Biol 2016;14:81–90.
[29] Gao R, Hu Y, Li Z, Sun J, Wang Q, Lin J, et al. Dissemination and mechanism for the MCR-1 colistin resistance. PLoS Pathog 2016;12:e1005957.
[30] Hancock RE. Cationic peptides: effectors in innate immunity and novel antimicrobials. Lancet Infect Dis 2001;1:156–64.
[31] Hancock RE, Chapple DS. Peptide antibiotics. Antimicrob Agents Chemother 1999;43:1317–23.
[32] Hua X, Liu L, Fang Y, Shi Q, Li X, Chen Q, et al. Colistin resistance in *Acinetobacter baumannii* MDR-ZJ06 revealed by a multiomics approach. Front Cell Infect Microbiol 2017;7:45.
[33] Ecker J, Liebisch G. Application of stable isotopes to investigate the metabolism of fatty acids, glycerophospholipid and sphingolipid species. Prog Lipid Res 2014;54:14–31.
[34] Scherer M, Bottcher A, Liebisch G. Lipid profiling of lipoproteins by electrospray ionization tandem mass spectrometry. Biochim Biophys Acta 2011;1811:918–24.
[35] Nikaido H. Molecular basis of bacterial outer membrane permeability revisited. Microbiol Mol Biol Rev 2003;67:593–656.
[36] Whitfield C, Trent MS. Biosynthesis and export of bacterial lipopolysaccharides. Annu Rev Biochem 2014;83:99–128.
[37] Eicher T, Cha HJ, Seeger MA, Brandstatter L, El-Delik J, Bohnert JA, et al. Transport of drugs by the multidrug transporter AcrB involves an access and a deep binding pocket that are separated by a switch-loop. Proc Natl Acad Sci U S A 2012;109:5687–92.
[38] Nikaido H, Takatsuka Y. Mechanisms of RND multidrug efflux pumps. Biochim Biophys Acta 2009;1794:769–81.
[39] Du D, Wang Z, James NR, Voss JE, Klimont E, Ohene-Agyei T, et al. Structure of the AcrAB–TolC multidrug efflux pump. Nature 2014;509:512–15.
[40] Baron SA, Rolain JM. Efflux pump inhibitor CCCP to rescue colistin susceptibility in *mcr-1* plasmid-mediated colistin-resistant strains and Gram-negative bacteria. J Antimicrob Chemother 2018;73:1862–71.
[41] Yun SH, Choi CW, Kwon SO, Park GW, Cho K, Kwon KH, et al. Quantitative proteomic analysis of cell wall and plasma membrane fractions from multidrug-resistant *Acinetobacter baumannii*. J Proteome Res 2011;10:459–69.
[42] Grundy FJ, Lehman SC, Henkin TM. The L box regulon: lysine sensing by leader RNAs of bacterial lysine biosynthesis genes. Proc Natl Acad Sci U S A 2003;100:12057–62.